

See discussions, stats, and author profiles for this publication at: <https://www.researchgate.net/publication/273327627>

Understanding the Retina: A Review of Computational Models of the Retina from the Single Cell to the Network Level

Article in *Critical Reviews in Biomedical Engineering* · January 2014

DOI: 10.1615/CritRevBiomedEng.2014011732 · Source: PubMed

CITATIONS

34

READS

3,721

7 authors, including:



Tianruo Guo
UNSW Sydney

72 PUBLICATIONS 537 CITATIONS

[SEE PROFILE](#)



David Tsai
UNSW Sydney

54 PUBLICATIONS 905 CITATIONS

[SEE PROFILE](#)



Siwei Bai
Technische Universität München

33 PUBLICATIONS 848 CITATIONS

[SEE PROFILE](#)



Socrates Dokos
UNSW Sydney

247 PUBLICATIONS 3,810 CITATIONS

[SEE PROFILE](#)

Understanding the Retina: A Review of Computational Models of the Retina from the Single Cell to the Network Level

Tianruo Guo,^{1,*} David Tsai,^{1,2,3} Siwei Bai,¹ John W. Morley,⁴ Gregg J. Suaning,¹ Nigel H. Lovell,¹ & Socrates Dokos^{1,5}

¹Graduate School of Biomedical Engineering, UNSW Australia, Sydney, NSW 2052, Australia; ²Howard Hughes Medical Institute, Biological Sciences, Columbia University, New York, NY; ³Bioelectronic Systems Lab, Electrical Engineering, Columbia University, New York, NY; ⁴School of Medicine, University of Western Sydney, Penrith, NSW, Australia; ⁵Department of Biomedical Engineering, Faculty of Engineering, Kuala Lumpur 50603, Malaysia

*Address all correspondence to: Tianruo Guo; Graduate School of Biomedical Engineering, UNSW Australia, Sydney, NSW 2052, Australia; Tel. +61-2-9385-9406 Fax +61-2-9663-2108; Email: t.guo@unsw.edu.au.

ABSTRACT: The vertebrate retina is a clearly organized signal-processing system. It contains more than 60 different types of neurons, arranged in three distinct neural layers. Each cell type is believed to serve unique role(s) in encoding visual information. While we now have a relatively good understanding of the constituent cell types in the retina and some general ideas of their connectivity, with few exceptions, how the retinal circuitry performs computation remains poorly understood. Computational modeling has been commonly used to study the retina from the single cell to the network level. In this article, we begin by reviewing retinal modeling strategies and existing models. We then discuss in detail the significance and limitations of these models, and finally, we provide suggestions for the future development of retinal neural modeling.

KEY WORDS: Retina, neuron, compartmental model, cascaded model, continuum model, network model.

I. INTRODUCTION

The retina is an elaborate architecture of neurons interconnected through gap junctions and synapses. At the outer retina, an array of rod and cone photoreceptors converts the incident light to neural responses. These signals then pass through approximately 10 types of cone cells and 1 type of rod bipolar cell before arriving at the output neurons in the inner retina—the retinal ganglion cells (RGCs). The approximately 12 types of RGCs then transmit the signals in the form of action potentials to the brain via the optic nerve. In addition to this vertical excitatory pathway, the retina also contains two lateral inhibitory pathways. In the outer retina, the horizontal cells provide inhibitory feedback to the photoreceptors, and inhibitory feed forward to the bipolar cells. In a similar scheme, the amacrine cells in the inner retina provide inhibition of the bipolar cells and the RGCs.¹

Very few neural circuits are comparable to this retinal system. First, the human retina has a clearly

organized architecture; every functional retinal layer can be physically identified. Secondly, input and output relationships in many retinal neurons and layers have been well characterized.^{2,3} Furthermore, this “one-directional” signal-processing system can be represented as an isolated circuit without considering efferent feedback from the brain. Existing anatomical and neurophysiological knowledge of retinal function has permitted computational models to reproduce aspects of retinal responses to either visual or artificial electric stimuli at various complexity levels. These models, in turn, have helped sharpen our understanding of the retina, particularly how intrinsic biophysical and anatomical properties at the cellular level, and integration of the synaptic inputs at the network scale, contribute to retinal function (Table 1). Indeed, over the past decades, computational models have been important for developing our understanding of the response dynamics and computations of single retinal neurons and their functional contributions in larger neural networks (Table 2).

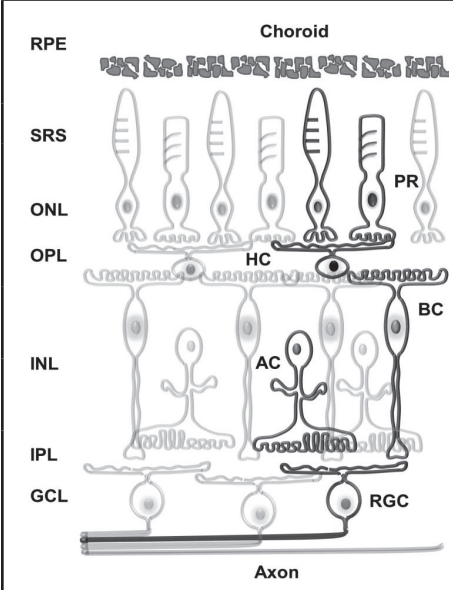
TABLE 1: Task-specific applications of various retinal neuron model types

| Task | Model type | Biological system |
|---------------------------------------|-----------------|---|
| Action potential initiation | II, III, IV | Rabbit RGC: ^{41,43,61} Mudpuppy RGC: ³² Tiger salamander RGC: ¹¹⁸ |
| Dendritic processing | II, III, VI | Rabbit starburst amacrine cell: ^{62,63,119} Tiger salamander amacrine cell: ⁵⁷ Rabbit OFF RGC: ⁴⁶ Rabbit direction selective RGC: ⁴⁷ Turtle direction selective RGC: ¹²⁰ Tiger salamander RGC: ¹⁰⁵ Cat ON alpha RGC: ¹²¹ Mudpuppy RGC: ¹²² |
| Effects of ionic channel distribution | I, II, VI | Tiger salamander RGC: ^{24,30,39} Bullfrogs rod photoreceptor: ¹²³ Rabbit ON and OFF RGC: ⁴⁸ Rabbit starburst amacrine cell: ¹¹⁹ Mouse dopaminergic amacrine cell: ²³ Tiger salamander amacrine cell: ⁵⁷ Goldfish horizontal cell: ¹⁸ |
| Effects of physical properties | II, III | Tiger salamander RGC: ^{30,44} Mudpuppy RGC: ¹²² Rabbit ON and OFF RGC: ^{30,42,45,46,48} Mouse ON and OFF RGC: ⁵⁰ Rabbit starburst amacrine cell: ^{62,119} Tiger salamander amacrine cell: ⁵⁷ |
| Effects of extracellular stimulation | II, III, IV, VI | Rabbit RGC: ⁴³ Rabbit retina: ^{33,61,76-79,81,124} Cat retina: ⁷⁷ Mouse and monkey RGC: ⁴² Mudpuppy retina: ⁴⁰ Tiger salamander RGC: ^{34,58,59,118,125} Primate retina: ¹⁰³ |
| Motion detection and anticipation | II, V, VI | Rabbit direction selective RGC: ⁴⁷ Tiger salamander and rabbit RGC: ⁹⁷ Cat RGC: ¹²⁶ Fly visual system: ¹²⁷ Tiger salamander/ rabbit retina: ⁵ Tiger salamander retina: ⁹⁸ |
| Effect of new ionic mechanisms | I, II, VI | Rabbit ON and OFF RGC: ^{26,45,46,48} Mouse ON and OFF RGC: ^{27,50} Mammalian rod photoreceptor: ¹⁰¹ Rat ON RGC: ⁴⁹ Mouse dopaminergic amacrine cell: ²² |

Despite these major advances, a large amount of retinal function remains to be described. For in-

stance, experimental studies increasingly indicate that the functions of many retinal neuronal types are

TABLE 2: Left panel: Schematic representation of the vertebrate retina. Right table: Different types of retinal neurons can be characterized into multiple model levels. I. single-compartment model, II. morphologically-realistic model, III. Block-compartment model and V. block-structured model. RR, CR, HC and BC models are largely limited to the single-compartment and block-compartment types due to their relatively simple morphology. Morphologically-complex neurons such as ACs and particularly RGCs are represented at all types. Block-structured formulation can reproduce the functional input/output relationship between light stimulus inputs and cell responses in nearly every retinal neuron type without considering the detailed biophysical structure of the neuron.

| <div> <div>Model type</div> <div>Neuron type</div> </div> | | I | II | III | V |
|--|-----------------------------|-------------------|---|-------------------------|-------------------|
| | | | | | |
|  | Rod photoreceptor (RR) | 15-17, 123 | | 35 | 90-92 |
| | Cone photoreceptor (CR) | 17, 101, 128, 129 | | 35, 65 | 85, 87-89 |
| | Horizontal cell (HC) | 18, 20, 130 | | 19, 65 | |
| | Bipolar cell (BC) | 21, 101 | | 64 | 100, 131 |
| | Amacrine cell (AC) | 22, 23, 101, 104 | 57, 119 | 56, 62, 63 | 132 |
| | Retinal ganglion cell (RGC) | 24-27, 101, 125 | 30, 32, 39-42, 44, 47-50, 58-61, 105, 122 | 30, 32, 33, 43, 49, 118 | 5, 82, 94-96, 133 |
| | | | | | |

more intricate than originally thought.^{2,4-8} Similarly, at the clinical frontiers, the mechanisms underlying the large diversity in retinal neuronal responses to artificial stimulations are still being investigated.⁹⁻¹²

On a micro scale, retinal neurons extract their preferred visual information, process this information (often with the help of other neurons), then transfer the results to downstream neurons. A single neuron can be represented by either a single-compartment model, a morphologically realistic model, or using a block-compartment approach, depending on the aims, complexities, and physiological assumptions on which the model is based. Such models integrate electrophysiological current/voltage-clamp recordings and biophysical principles into a mechanistic understanding of individual neuronal properties, reconstructing ionic mechanisms hidden in the data, as well as utilizing new experimental information to improve existing model structures.

On a larger scale, visual information is arrayed across large inhomogeneous populations of neurons within each retinal layer. One approach to representing such a neuronal networks involves bringing together individual neurons, each being a complete model capable of stand-alone execution, and connecting them using the computational representation of synapses. As such, these models are generally mechanistically detailed but are computationally expensive to run. Alternatively, functional block-structured models could also be used to construct large-scale models of the retina. Unlike the aforementioned approach, these models aim to capture only the input–output relationship of the neuron/network by treating the constituent neurons as black boxes.¹³ By omitting neuronal morphological details, and often the associated ionic biophysics as well, these approaches have the advantage of computational efficiency. These large-scale tissue- or network-based models have been used to investigate how each retinal neuron contributes to a

particular sub-circuit or the entire retinal tissue and how they work together to collectively encode visual input. Irrespective of the modeling technique, they offer a better understanding of the growing amount of experimentally recorded retinal responses to light or electrical stimuli and can be used to make testable predictions. For clinical applications, some of these models also provide valuable insights into the development of effective stimulation strategies for visual prostheses.¹⁴ In this review, we examine the current state-of-the-art of computational models of the neural retina across different scales, and we discuss their advantages, limitations and future potential.

II. SINGLE-COMPARTMENT MODELS

Single-compartment models, also known as “point models,” (Fig. 1, type I) have been used to simulate nearly all retinal neuron types, including photoreceptors,^{15–17} horizontal cells,^{18–20} bipolar cells,²¹ amacrine cells,^{22,23} and a range of RGC types.^{24–27} These models approximate the structure of the neural excitable membrane using capacitance to mimic the membrane phospholipid bilayer, in parallel with several conductors to mimic transmembrane channels composed of proteins. The relationship between the transmembrane potential and membrane currents is described by the following ordinary differential equation (ODE):

$$J_m = C_m \frac{dV_m}{dt} + J_{ion} + J_{stim} = 0, \quad (1)$$

where J_m denotes total membrane current density (current per unit membrane area), V_m represents membrane potential, C_m represents membrane capacitance per unit area, and J_{ion} represents the total ionic current density.²⁸ A single-compartment model assumes no net current across the cell membrane ($J_m = 0$), because all current flowing through the ionic channels charges the membrane capacitance. This is also known as the space-clamped condition. Furthermore, the neuron may be activated by an intracellular stimulus current density (J_{stim}) delivered into the cell to mimic experimental manipulation during intracellular recordings.

Because ionic mechanisms of retinal neurons are far more complex than those of the classic Hodgkin-

Huxley ionic model of the giant axon of squid,²⁹ many modelers have chosen to modify the classic model and have extended it to replicate the known ionic mechanisms in various retinal neurons. Among the first ionic models developed for the retina were those for the RGCs. Their all-or-none spiking behaviors closely follow the classical notion of neurons; thus, they are easily modeled by modifying existing Hodgkin–Huxley-type formulations. A landmark in RGC modeling was the Fohlmeister–Coleman–Miller (FCM) formulation.^{24,25,30} This model is based on voltage clamp studies in the tiger salamander, and it contains five intrinsic ion currents underlying RGC spiking. Prior to these studies, experimental knowledge of detailed ion channel kinetics or their neuronal distribution was rarely used in retinal neural modeling. The FCM model also includes intracellular calcium dynamics responsible for temporal spiking properties. With more optimized Na^+ and K^+ gating kinetics, the FCM model demonstrates many advantages over the original Hodgkin–Huxley formulation in terms of impulse encoding flexibility,³¹ revealing its ability to reconstructing a large range of neuronal spiking behaviors. Since its publication, this model and its derivatives have led to further quantitative understanding of many dynamical phenomena in RGCs, including spike-frequency adaptation,²⁴ rebound activation,^{26,27} burst firing,²⁷ and subthreshold activities.²⁷

Moreover, the single-compartment FCM model was also validated in higher-dimensional simulations with detailed anatomical information or network interactions. To the best of our knowledge, Fig. 2 illustrates nearly all applications and extensions based on FCM formulations in the last two decades. Its morphology-, tissue- and network-based extensions are discussed in the following sections.

Despite the reported functional significance of all five ionic currents in the FCM model, relatively simpler ionic models are still used to study specific RGC response properties when accurate impulse generation are required,^{32–34} as well as for other retinal neurons (e.g., photoreceptors or bipolar cells).^{18,35}

The advantage of simplicity in a single-compartment model is also its weakness. Certain disparities between the single-compartment FCM

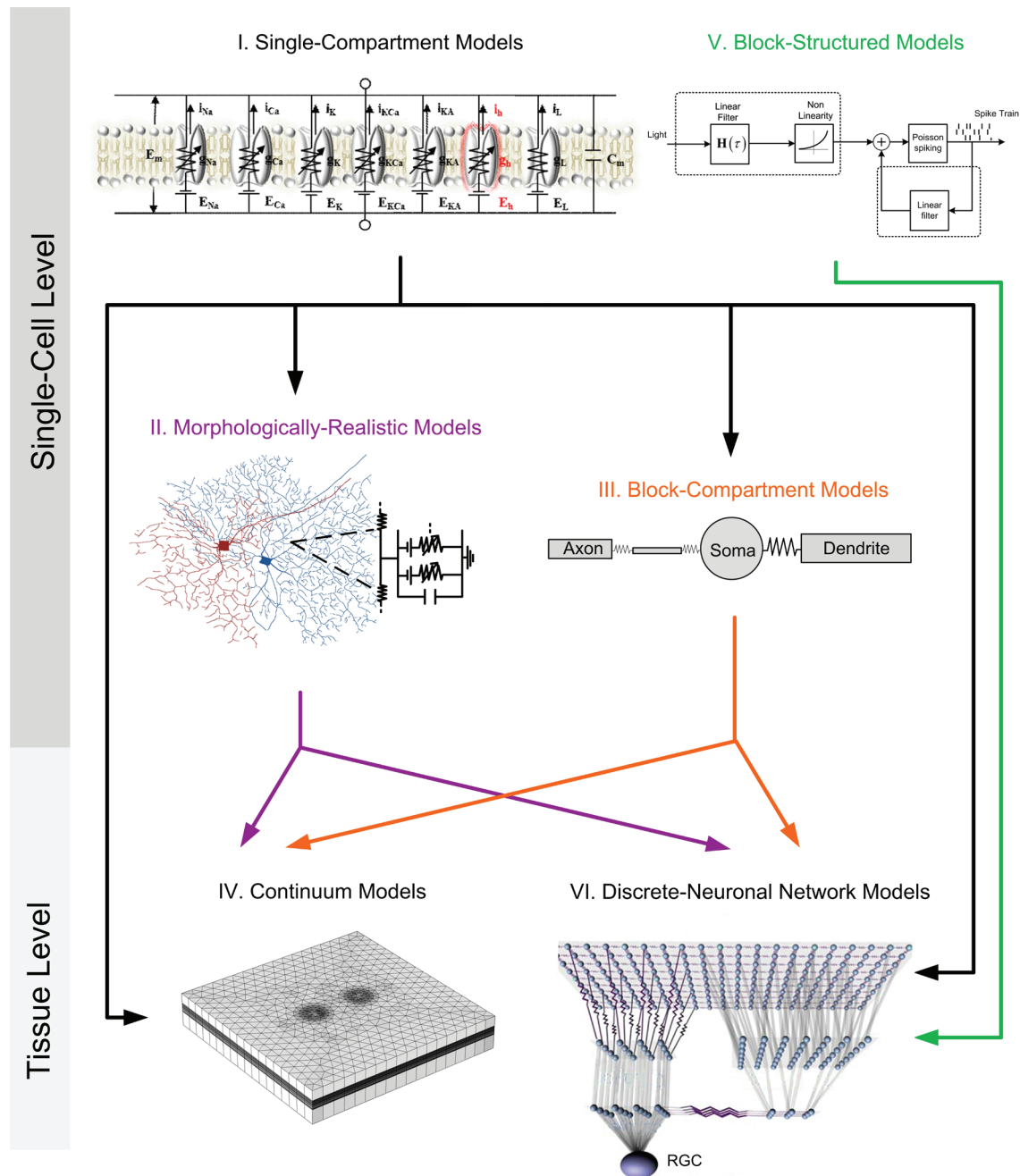


FIG 1: Six types of computational models typically used in retinal neuron modeling. I. Single-compartment models, II. Morphologically realistic models, III. Block-compartment models, IV. Continuum models, V. Block-structured models, and VI. Discrete-neuronal network models, adapted from Pubio *et al.*¹⁰¹ Depending on the study aim, a single-compartment neuron model can be extended to any biophysical model type (II, III, IV, VI), by adding new assumptions such as anatomical structure, synaptic or inter-neuron coupling information. Conductance-based models (i.e., types I, II, and III) can be used as individual neuron elements in both continuum models and discrete-network models. Block-structured models are often used in building retinal networks or localized subcircuits. Large-scale network models can capture the essential function of photoreceptors, bipolar cells and RGCs, as well as the contribution of retinal heterogeneity in visual information processing.

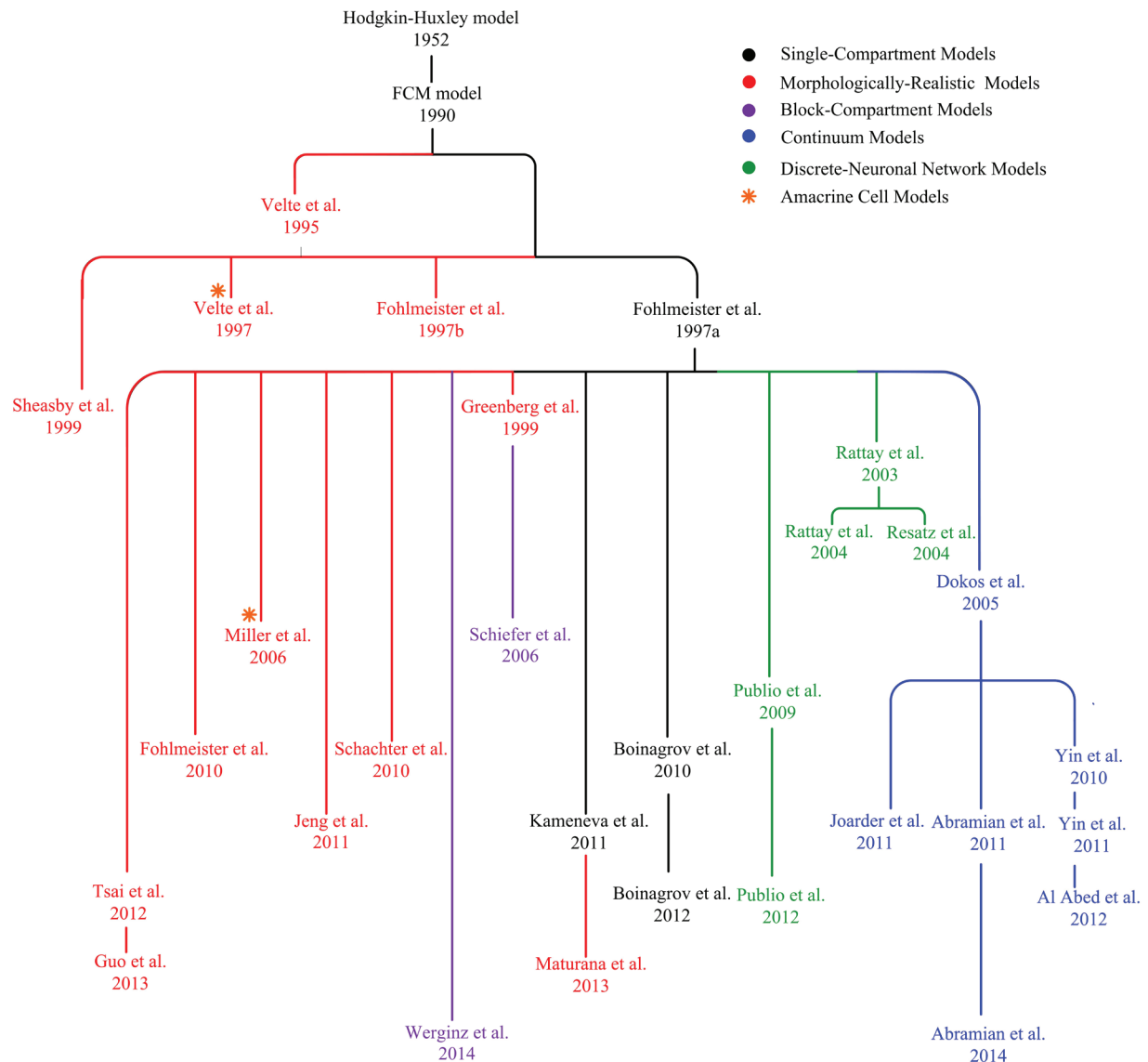


FIG 2: Fohlmeister-Coleman-Miller (FCM) model family. The FCM model and its extensions have been successfully used for RGC or amacrine cell model reconstruction. Existing FCM type models are widely applied in morphologically-realistic modeling (red) to study the effect of non-uniform channel distribution or regional interaction. Single-compartment FCM models (black) focus on studying the contribution of each active conductance and integrating new identified ionic currents into an existing model framework. The FCM model is also widely used as individual RGC elements in continuum tissue-based (blue) and retinal circuit models (green), by adding the information of retinal layers and network interactions.

model and known biological RGC behavior cannot be reconciled by optimizing the model parameters alone.²⁴ Having additional neuronal compartments that differ in both size and ionic channel density could also produce more realistic spike generation

and propagation.³² Recent brain-cell studies suggest that models cannot capture subtle response characteristics, such as fast depolarization during action potentials, without incorporating representations of axons and dendrites and the propagation of cur-

rent along these neurites.^{36–38} Therefore, rather than simply incorporating intrinsic properties at a single point, the spatial anatomical information and ionic channel distribution are also required for accurate neuronal modeling.

III. MORPHOLOGICALLY REALISTIC MODELS

To create models that represents their biological counterpart more closely, morphologically realistic models (Fig. 1, type II) have been developed based on detailed anatomical representations of the physical components in biological neurons, including soma, axon initial segment (AIS), axon hillock (AH), distal axon, and dendrites. Such models are ideal for studying how cell morphologies and non-uniform distributions of ionic channels contribute to neuronal response dynamics and how these affect function. Morphologically realistic models provide a good approximation of biological neuronal behaviour, and they have been largely used to build structurally “complex” retinal neurons such as amacrine cells and RGCs. These models sometimes include more than 1000 morphological segments to ensure accurate spatial resolution.³⁹

In morphological cable models, membrane potential is both space- and time-dependent, necessitating the modification of eq. (1) as follows:

$$I_m = \frac{\partial}{\partial s} (\sigma_i \frac{\partial V_m}{\partial s}) = \beta \left(C_m \frac{\partial V_m}{\partial t} + J_{ion} + J_{stim} \right), \quad (2)$$

where I_m is the volumetric current density (current per unit volume), s is the arc-length distance along the neuron, σ_i is the intracellular conductivity, and β is the local surface to volume ratio ($\beta=2/r$ for a circular cross-section neural region of radius r).

In practice, Eq. (2) is approximated by separating the neuron into multiple discrete regions; each region associates with its own ionic properties and is connected with neighboring compartments by axial conductors. The more compartments used, the more closely the model simulates the biological neuron.

An advantage of this type of model is that it can also simulate cell responses to extracellular electrical stimulation, as opposed to only intracellular stimulation in the single-compartment model

because a single-compartment model assumes no net current across the cell membrane. In this situation, membrane potential is calculated by taking the difference between intracellular potential V_i and extracellular potential V_e ,

$$V_m = V_i - V_e, \quad (3)$$

where V_i is derived from

$$\frac{\partial}{\partial s} (\sigma_i \frac{\partial V_i}{\partial s}) = \beta \left(C_m \frac{\partial V_m}{\partial t} + J_{ion} \right) \quad (4)$$

and the extracellular voltage distribution can be simulated by either a monopolar point source^{40,41} or a disk electrode,^{40–42} respectively, modeled as

$$V_e = \rho_e I / 4\pi r \quad (5)$$

$$\text{or } V_e = \frac{2IR_s}{\pi} \arcsin \left(\frac{2R}{\sqrt{(a-R)^2 + z^2} + \sqrt{(a+R)^2 + z^2}} \right), \quad (6)$$

where ρ_e denotes the resistivity of the retinal extracellular solution, I is the extracellular stimulus current, r is the distance between the stimulating electrode and the point at which the voltage is being computed, a and z are the radial and axial distances, respectively, from the center of the disk for $z \neq 0$, R is the radius of the disk, and R_s is the electrode transfer resistance. Notably, Eqs. (5) and (6) are applicable to infinite and semi-infinite homogeneous media, respectively.

In some cases, the extracellular voltage distribution has been coupled to the local membrane potential,⁴³ given by

$$\frac{\partial}{\partial s} (-\sigma_e \frac{\partial V_e}{\partial s}) = \beta \left(C_m \frac{\partial V_m}{\partial t} + J_{ion} \right), \quad (7)$$

where σ_e denotes the extracellular conductivity.

Neuronal morphology can influence the flow of intracellular currents between neighboring compartments through the cell membrane and by intracellular conductance. As a result, morphology may also contribute to the unique spiking behavior of different RGC types.⁴⁴ Although dendritic morphologies and stratifications of RGCs have been examined extensively, their contribution to RGC spiking patterns is not well understood, owing to the difficulty of isolating and manipulating such properties in the

experimental preparation. However, the morphologically realistic modeling approach can quantitatively control a variety of cellular properties, including morphology, and can isolate their contributions in shaping firing patterns.^{45,46}

Notable examples of morphologically realistic retinal neuron modeling include (1) the FCM (1997) model,³⁰ which is the first morphologically detailed RGC formulation able to closely reconstruct action potential shapes and spiking properties; (2) the Sheasby-Fohlmeister (1999) realistic RGC encoder,⁴⁴ which has been used to explore the effect of regional ionic channel distributions along the cellular morphology; (3) the Schachter *et al.* (2010) model,⁴⁷ which explained the mechanisms of active dendritic processing of synaptic inputs in direction-sensitive RGCs; and (4) the Jeng *et al.* (2011) sodium-channel-band model,⁴¹ which enabled the determination of the factors underlying action potential initiation site in response to electrical stimulation of RGCs.

These morphologically detailed modeling approaches offer important information on how their channel distributions influence RGC firing patterns and how the interaction between different cell regions influences the neural coding. Recently, Guo *et al.*⁴⁸ presented a cell-specific realistic-morphology approach for ON, OFF, and OFF-parasol RGCs. The recent morphologically realistic model of Abbas *et al.*⁴⁹ suggested that dendritic ionic channels provide RGCs with the ability to code “looming” motion. Another recent study by Maturana *et al.*⁵⁰ focused on how physical properties of RGCs contribute to their specific spiking response patterns in response to electrical stimulation.

Experimental findings have also suggested that RGC dendrites exhibit regenerative spikes, as opposed to being simply passive neurites.^{51–53} The detailed dendritic structure of morphologically realistic models can provide the framework for investigating dendritic signal processing because the physical properties can be precisely controlled in these models. Furthermore, the dendritic active conductances can be modulated *in silico*, to study their effects on RGC spiking properties.⁴⁶ In summary, the realistic neuron modeling approach provides a promising tool for studying soma–dendrite interactions, assisting in interpreting experimental studies in dendritic patch-

clamp recordings, fluorescent imaging, and immunocytochemical channel localization techniques.

Other than their application to the RGCs, morphologically realistic models have also been applied to amacrine cells, which also demonstrate a large diversity in functional properties.^{54,55} A morphologically realistic starburst amacrine cell model was developed by Fohlmeister *et al.* to study the mechanisms underlying local dendritic processing.²⁵ By testing different artificial morphologies, another amacrine modeling study by Tukker *et al.*⁵⁶ suggested that directional sensitivity may mainly depend on a sufficient number of synaptic inputs at the distal dendrites rather than the dendritic morphology itself. Another amacrine modeling study by Miller *et al.* (2006) suggested that various amacrine cell-spiking properties could be reproduced by a RGC model with minimal parameter adjustment,⁵⁷ revealing the close ionic relationships between some amacrine cells and RGCs.

Although certain morphologically realistic retinal neuron models have also been used in constructing accurate models of local circuits or the whole-tissue retina to study neuronal interactions during electrical stimulation,^{40,58–60} their huge computational demand has resulted in their restricted use for population-based simulations, especially in large-scale network modeling.

IV. BLOCK-COMPARTMENT MODELS

An alternative modeling strategy, block-compartment modeling (Fig. 1, type III) represents only a few neuronal regions, compromising between computational efficiency and biological realism. These models can be considered simplified versions of the morphologically realistic approach, extracting the most essential anatomical information to provide high computational efficiency with minimal neural structure.

The simplest model in this genre is a two-compartment system coupled by a linear conductor, representing a soma and a dendritic or axonal compartment. In this way, Eq. (2) can be updated as follows:

$$\begin{aligned}\frac{G_c}{p}(V_x - V_s) &= C_m \frac{dV_s}{dt} + J_{ion,s} \\ \frac{G_c}{1-p}(V_s - V_x) &= C_m \frac{dV_x}{dt} + J_{ion,x}\end{aligned}\quad (8)$$

where V_s and V_x represent the membrane potential in the soma and connected compartment respectively, G_c is the coupling conductance between compartments, p is the percentage of the cell membrane area taken up by the soma, and $J_{ion,s}$ and $J_{ion,x}$ are the membrane potentials of the soma and connected compartment, respectively.

This morphology-reducing process depends largely on the motivation of specific studies as well as the ionic mechanisms involved. Previous findings have suggested that reasonably realistic RGC spiking patterns, comparable to experimental recordings and simulations from morphologically realistic models, can be obtained using only four neuronal compartments (dendrites, soma, thin segments, and axons).³⁰ A single, unbranched, dendritic compartment, which allows regionally specific activation of individual channel subtypes, has been shown to be sufficient to elicit summation of excitatory postsynaptic potentials (EPSPs) in RGCs.⁴⁹ In addition, a simplified axonal activation model was able to successfully predict RGC experimental threshold profiles as well as the initial activation location in response to electrical stimulation.⁴³ In another model investigating the origin of AP initiation in RGCs, the dendrites were reduced to unbranched cables of uniform diameter.³² Another such simplified RGC-structure model was used to investigate how epiretinal electrical stimulation could result in the production of punctate phosphenes as opposed to diffuse or streaked perceptions that would be consistent with the recruitment of axons from distant RGCs.⁶¹ In a more recent tissue-based retinal model, each point in the RGC layer was represented by an active soma and a passive dendritic compartment, with a synaptic input into dendrites included to approximate the underlying neural structure.³³

Apart from RGC models, equivalent cable representations have also been used to simulate starburst amacrine cells.^{56,62,63} These models incorporate various levels of simplified cylindrical dendritic structures, and have been helpful in elucidating the influence of morphological structure on the mechanisms underlying directional sensitivity in starburst amacrine cell networks.

Block-compartment models have also been applied to morphologically simple neurons such

as photoreceptors,³⁵ bipolar cells,⁶⁴ and horizontal cells^{19,65} (Table 2). Most of these retinal neuron types do not demonstrate significant morphological diversity, and they require only a simple physical structure such as a cylindrical soma connected to an axon terminal.

One question that must be answered in block-compartment models is this: To what extent can retinal neurons be simplified without compromising realistic cell behavior? A general principle is that models should be at the simplest level required to reproduce desired behavior of a physical system. This also raises another question: To what extent does neural morphology contribute to its response? A recent study by Guo *et al.*⁴⁵ provided an example showing the contribution of morphology to cell responses for which RGC models could reproduce distinct variations in spiking patterns in response to intracellular current injection by solely varying their morphology, with all biophysical parameters describing voltage-gated channel kinetics and distributions remaining unchanged. In addition, the spatial distribution of membrane ion channel densities among the various neural compartments also contributes to the neuronal response.

Because there is no generally clear simplification approach in block-compartment neural modeling, an alternative approach comprises iterative morphometric simplification wherein the reducing process is stopped when the model fails to reproduce biological cell responses. Although the influence of systematic morphologic perturbations in neuronal behavior has been reported in several brain cell studies,^{37,66} no similar approach has yet been used in retinal neuron modeling. A morphometric simulator was developed recently to study how dendritic intersections, branching points, and terminal tips contribute to correct classification of RGC images.⁶⁷ One could imagine, for example, the integration of such a morphometric generator into a modeling framework to create a platform for exploring the ramifications of RGC morphological variations.^{68–70}

V. CONTINUUM MODELS

Continuum models (Fig. 1, type IV) have been used to simulate the response of bulk retinal tis-

sue activation in an averaged spatial sense, without explicit representation of the constituent neurons. Continuum bidomain (intra- and extracellular domains) formulations have proven useful in cardiac^{71,72} and neural tissue simulation.^{73,74} These models are able to simulate bulk active or passive current flow across neuronal membranes into the extracellular space, perturbing the extracellular potential, as has been observed experimentally dating back several decades.⁷⁵ This advantage allows the continuum bidomain approach to be an ideal tool for simulating the spatial extent of retinal activation due to extracellular electrical stimulation (Table 1), as well as investigate the influence of electrode configuration, position, and stimulus parameters on retinal tissue responses.

In continuum retinal models, the dynamics of both extracellular and intracellular potentials are considered:

$$I_m = \nabla \cdot (-\sigma_e \nabla V_e) = \nabla \cdot (\sigma_i \nabla V_i) = \beta \left(C_m \frac{\partial V_m}{\partial t} + J_{ion} \right), \quad (9)$$

where $V_m = V_i - V_e$, σ_e is the extracellular conductivity. Some formulations adopt a “pseudo-bidomain” approach⁷⁶ by tying the intracellular potential to a remote resting potential:

$$I_m = \nabla \cdot (-\sigma_e \nabla V_e) = g_r (V_r - V_i), \quad (10)$$

where V_r is the intracellular potential of a “remote” neural compartment and g_r is an intracellular conductance tying the intracellular potential to this remote compartment. The effect of the latter parameter is to prevent the intracellular potential from floating freely with changing extracellular potential, due to an applied stimulus.

The first such model of retinal electric simulation was the Dokos *et al.* (2005) model, comprising a vitreous and an active RGC layer.⁷⁷ It represented a “genuine bidomain” formulation (i.e., Eq. (9)) and was used to simulate the retinal response to a bipolar electrode configuration using various stimulus waveforms. This model was then extended by adding further retinal layers, including a passive inner plexiform layer, nuclear layer, subretinal space, retinal pigment epithelium, and choroid.⁷⁸ A similar model was also used to investigate the threshold of neuronal

activation and the spatial extent of activation, thus providing valuable information regarding stimulus thresholds and localization of activation.⁴³ A more recent retinal model by Abramian *et al.* was used to investigate multi-electrode array stimulation.⁷⁹ This model examined the advantages of so-called “quasi-monopolar” stimulation compared to bipolar or monopolar stimulation, combining the low thresholds of monopolar stimulations with the focal spatial activation of hexapolar configurations.⁸⁰

Continuum models can be also be further extended by adding network effects, as in the retinal model of Yin *et al.*,⁷⁶ which included excitatory input from bipolar cells and inhibitory input from wide-field amacrine cells. This model was subsequently refined by adding a dendritic compartment and synaptic currents to account for presynaptic influences on RGC activation.³³ A further model utilizing microcircuitry of the ON cone pathway was formulated to investigate the network response to large and small spots of light.⁸¹

These retinal models can be widely used to study the spatial activation profile of electrical stimulation. They provide a promising modeling framework that could be easily extended by incorporating newly identified ionic currents and synaptic connections.

VI. BLOCK-STRUCTURED MODEL OF RETINAL FUNCTION

Apart from the aforementioned biophysically detailed models, a black-box approach can be used to represent the retinal network. The goal of these models is to capture statistical relationships between light stimuli and cell firing rates without describing detailed neural structure, biophysics, and network connectivity. A popular approach for implementing these block-structured models, also known as “cascaded models,” (Fig. 1, type V) involves representing the retina as a series of linear and nonlinear temporal filter elements.^{82,83} These models can closely reproduce responses of the retina to simple laboratory light stimuli using only a few free parameters. Block-structured models do not attempt to accurately reconstruct biophysical aspects of real retinal neurons; however, they can provide enough overall functional characteristics to cover both the computational aspects of

individual retinal neurons and the collective capabilities of large-scale neural networks. Thus, they are very popular in modeling local neural circuits⁸⁴ or the whole retinal network^{85,86} (Fig. 1 VII).

Block-structured models have largely been used to simulate behavioral characteristics of outer retinal neurons, the cones^{87–89} and rods^{90,91} (Table 2). Despite their high degree of simplicity, these phenomenological models have been successfully applied to investigate specific physiological mechanisms, including those underlying normal and abnormal rod-receptor activity affected by retinodegenerative disease,⁹² as well as nonlinear synaptic dynamics between photoreceptors and downstream neurons.⁹³

In block-structured models, specific neural spiking behaviors have been reproduced by their unique transfer functions, characterizing linear and nonlinear spatial summation mechanisms in various types of RGCs in cat retina.^{94,95} A generic spike-train simulator was also able to accurately reconstruct spiking responses in a large range of functionally-identified RGCs from different species.⁹⁶

These functional models have also been popular for studying retinal motion detection and anticipation (Table 1). In one study, motion extrapolation in many species was reproduced by block structures representing the spatially extended receptive field, the biphasic temporal response and a nonlinear contrast-gain control.⁹⁷ Another block-structured model of object motion sensitive circuitry was able to predict the neuronal response at each stage of the circuit,⁹⁸ revealing the contribution of specific retinal interneurons in global motion detection.

As mentioned above, numerous successful blocked-structured models have defined various retinal pathways, receptive fields and stimulus-response transfer functions. However, the mechanisms underlying visual information processing may be far more complex than a series of temporal filters. Functional computation in a real retinal neuron is also highly related to its physical structure, ionic channel expressions, and synaptic interactions. In this regard, block-structured models are not ideal for relating high-level response characteristics of neurons, or of a neural network, to the underlying mechanisms from which these characteristics arise. Block-structured models also cannot easily simulate

cellular responses to extracellular or intracellular electrical stimulation, limiting their utility in modeling retinal activation by artificial electric stimulation, as in visual prostheses.

VII. DISCRETE-NEURONAL NETWORK MODELS

The retinal network can also be simulated by grouping discrete retinal neuron elements, based on techniques described in sections I or II for instance, with excitatory and inhibitory synaptic interactions. In addition to neural properties and stimulus parameters, these discrete-neuronal network models (Fig. 1, type VI) also take into consideration the influence of forward and feedback connections among neurons, as well as the physical architecture of the retina.

A discrete-neuronal network model can represent either the entire retinal structure⁸⁶ or a retinal subsystem, including the cone-rod network,⁹⁹ the rod-bipolar network,¹⁰⁰ the cone-horizontal cell circuit,⁶⁵ the horizontal cell layer,¹⁹ the rod pathway,¹⁰¹ the cone pathway,^{85,102,103} the amacrine network,¹⁰⁴ bipolar-RGC interactions,⁵⁹ and the RGC layer¹⁰⁵ (Fig. 3).

Most discrete-neuronal network models do not focus on physiological precision in individual neurons but on the functional output of the retina on a large scale. They are generally constructed using non-biophysical neuron formulations such as cascaded models. This allows them to include a large number of cells with multiple visual pathways rather than specific local microcircuits while remaining computationally tractable. As such, these models can be very effective for investigating complex neural networks containing a large number of cells of different types. For example, one large-scale retinal model, comprising up to 10^5 neuron elements, was able to achieve both accurate physiological behavior as well as reasonable computational efficiency.⁸⁶ Another study examined the contribution of different cell subclasses in a large RGC population, facilitating the development of testable population-based hypotheses.¹⁰⁶ In addition, these functional network models have also been used to provide a comprehensive description of electroretinogram (ERG) generation using only local rod-bipolar circuits.¹⁰⁰

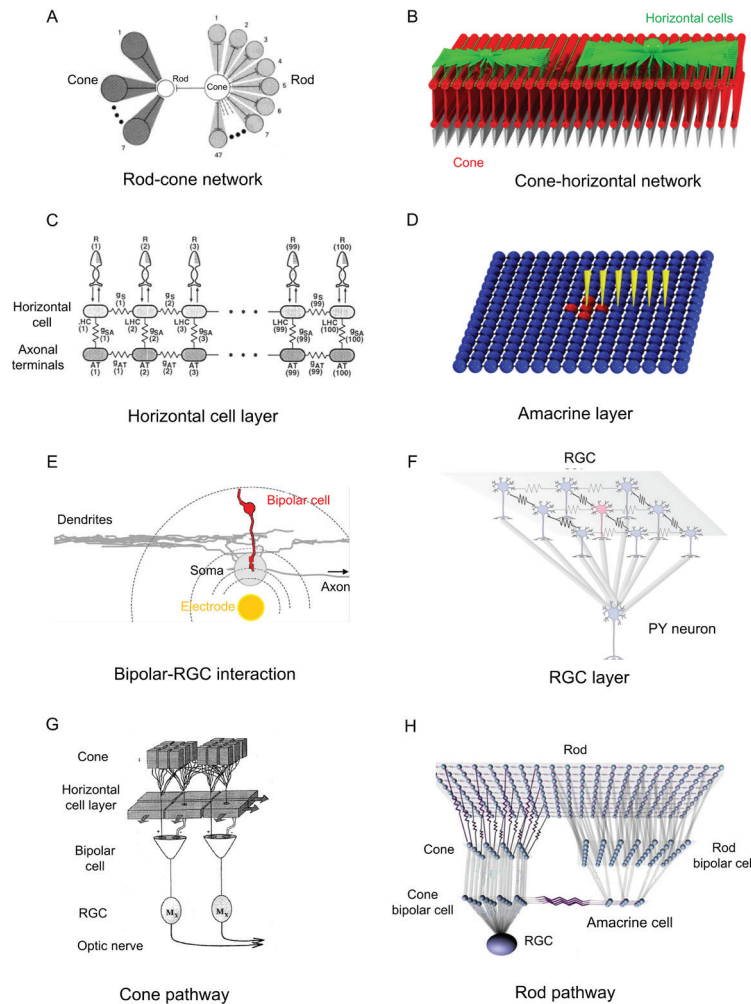


FIG 3: Examples of retinal network models. **(A)** Cone–rod network, based on Rallian static cable equations.¹³⁷ 48 rods converge on each cone and each cone connects to 8 other cones via gap junctions. Each rod or cone model is represented by a spherical soma and a cylindrical axonal segment. Rod-cone basal processes and cone-cone basal processes are modeled by cable segments with different terminating gap junction conductances, adapted from Smith *et al.*⁹⁹ **(B)** Cone-horizontal circuit, consisting of a 26×26 cone (red) array and two different types of horizontal cells (green). Both cones and horizontal cells are approximated using block-compartment models. Each horizontal cell is in contact with multiple cones through their dendritic terminals, adapted from Smith.⁶⁵ **(C)** 1-D horizontal cell layer, consisting of 100 horizontal cell elements with a Hodgkin–Huxley-type somatic compartment and a linear RC axonal compartment. Different gap junction values are employed between neighboring somas and those between axonal terminals, adapted from Usui *et al.*¹⁹ **(D)** Amacrine network, reconstructed using a 15×15 array of Hodgkin–Huxley-type spherical isopotential somas with presynaptic terminals and synapses, adapted from Smith and Vardi.¹⁰⁴ **(E)** Local bipolar-RGC circuit, coupled by a morphologically-detailed RGC and bipolar cell models, adapted from Rattay *et al.*⁵⁹ **(F)** RGC layer, reconstructed using a 3×3 array of morphologically-detailed RGC models, with dendrodendritic gap junctions between neighboring cells. Each RGC reproduces an excitatory chemical synapse with a pyramidal (PY) cell from the lateral geniculate nucleus (LGN) of the thalamus, adapted from Publio *et al.*¹⁰⁵ **(G)** Cone-pathway circuit reconstructed with a series of block-structured models. There is approximately one RGC output for every nine cones, adapted from Shah and Levine.⁸⁸ **(H)** Rod pathway circuit, built using connected single-compartment ionic models of rod/cone photoreceptors, bipolar cells, amacrine cells and RGCs coupled with electrical and chemical synapses, adapted from Publio *et al.*¹⁰¹

They can also qualitatively explain various types of adaptation during visual information processing.⁵

Some discrete-neuronal network models also incorporate detailed descriptions of retinal connectivity in successive neural layers, with these connections modeled by conductance-based formulations with a full set of cellular and synaptic parameters. For example, the model of Cottaris *et al.*¹⁰³ was developed by including both ON and OFF cone pathways with nine types of retinal neurons. The model was able to characterize the spatiotemporal activation of the retinal network during epiretinal electric stimulation, demonstrating the potential contribution of this artificial stimulus mode in shaping visual input to the cortex. Another detailed network model by Hennig *et al.*¹⁰⁷ was used to test the influence of various retinal cell classes and subcircuits on the unique response pattern in each identified RGC type. Although conductance-based formulations used in these models were not based on detailed ionic mechanisms in individual neurons, they were still able to achieve a high degree of accuracy in neural outputs at different levels of the retinal circuit.¹⁰⁸

It is important to note that detailed single-cell ionic models or morphologically realistic models are not typically used in the discrete-neuronal network modeling for computational efficiency reasons, except for studies focusing on local microcircuit stimulation. Examples of the latter include (1) ionic models of rod/cone photoreceptors, bipolar cells, amacrine cells, and RGCs in an accurate network retinal description;¹⁰¹ (2) a modified Hodgkin-Huxley model to represent single neurons in an amacrine cell network;¹⁰⁴ (3) a morphological RGC model in a local bipolar-RGC circuit;^{58,60} and (4) a recent model of the RGC layer represented by morphologically realistic models with dendro-dendritic gap junctions.¹⁰⁵

VIII. OUTLOOK ON RETINAL MODELING

Among all retinal neuron types, the mechanisms underlying morphologically complex retinal neurons such as amacrine cells or RGCs remain unclear (for a review, see Masland²). There are more than 13 identified amacrine cell types and 12 RGCs types in mammalian retina. A definitive description of

these cells has not yet been made due to their rich diversity in both intrinsic electrophysiological and morphological properties. Limited experimental information on ion-channel kinetics and distributions in identified cell types also makes cell-type-specific model parameter optimization a difficult task. Prior models of these neurons (Table 2) have been largely limited to identification of individual types, regardless of the diversity of the cellular morphology and membrane channel distributions/kinetics in each cellular region, despite the fact that the correlation between neuronal function and inherent biophysical properties is highly significant.^{68,69} On the other hand, despite far less morphological diversity, debate continues about the functional classification and mechanisms of horizontal cells and bipolar cells. New knowledge about these “pre-processing” neurons continues to be revealed.^{109–113} Therefore, further model validation based on new experimental evidence is still required to quantitatively identify and define these cells.

At the single-cell level, the composition of ion channels in retinal neuron models continues to be refined. The initial FCM model with five active membrane currents appears to be oversimplified; new ionic channel in retinal neurons have been identified.^{114–116} Ionic channel formulations are generally based on voltage-clamp experimental data, and the properties of these new currents and their regional distributions in different neuron types may significantly contribute to the overall neural response. With the likely discovery of more ionic mechanisms in retinal neurons, there still remains substantial room for improvement of the single-cell models.

In whole-retina models, the functional significance of cell morphology has not been systematically studied, even though its importance has been recognized in brain neuron network modeling.¹¹⁷ Why do retinal neurons present a large range of morphological diversity? It appears that morphological factors play some role in mediating neuronal function. Cell-specific morphological information will therefore play an increasing role in the development of future tissue- or network-based models of retinal function.

Finally, the ability of existing retinal neuron models to simultaneously reproduce experimental

data under a large range of diverse experimental conditions remains unclear. Most of the retinal model parameters need to be adjusted and optimized to reproduce additional behavior and datasets not included in the original model formulation. Thus, an unsupervised and computationally effective model optimization toolbox, which can simultaneously fit multiple datasets, will be a major contribution to this area.

ACKNOWLEDGMENT

The authors thank Mr. Erick Javier Argüello Prada for his thoughtful comments on parts of this manuscript. We also thank Dr. Shijie Yin for his hand-drawn diagram of the retina. This study was supported by the Australian Research Council (ARC) through a Special Research Initiative in Bionic Vision Science and Technology grant to Bionic Vision Australia (BVA)

REFERENCES

1. Masland RH. The fundamental plan of the retina. *Nature Neurosci.* 2001;4(9):877–86.
2. Masland RH. The neuronal organization of the retina. *Neuron.* 2012;76(2):266–86.
3. Roska B, Meister M. The retina dissects visual scenes into distinct features In: Werner JS, Chalupa LM, editors. *The new visual neurosciences*. London: MIT Press; 2014. p. 163–82.
4. Zhang YF, Kim IJ, Sanes JR, Meister M. The most numerous ganglion cell type of the mouse retina is a selective feature detector. *P Natl Acad Sci USA.* 2012;109(36):E2391–E8.
5. Hosoya T, Baccus SA, Meister M. Dynamic predictive coding by the retina. *Nature.* 2005;436(7047):71–7.
6. Freed M. Parallel cone bipolar pathways to a ganglion cell use different rates and amplitudes of quantal excitations. *Invest Ophth Vis Sci.* 2001;42(4):S519–S.
7. Fried SI, Munch TA, Werblin FS. Mechanisms and circuitry underlying directional selectivity in the retina. *Nature.* 2002;420(6914):411–4.
8. Golisch T, Meister M. Eye smarter than scientists believed: neural computations in circuits of the retina. *Neuron.* 2010;65(2):150–64.
9. Twyford P, Cai C, Fried S. Differential responses to high-frequency electrical stimulation in ON and OFF retinal ganglion cells. *J Neural Eng.* 2014;11(2):025001.
10. Freeman DK, Rizzo JF, Fried SI. Encoding visual information. Freeman DK, Rizzo JF, Fried SI. Encoding visual information in retinal ganglion cells with prosthetic stimulation. *J Neural Eng.* 2011;8(3): 035005.
11. Felsen G, Dan Y. A natural approach to studying vision. *Nature Neurosci.* 2005;8(12):1643–6.
12. Tsai D, Morley JW, Suaning GJ, Lovell NH. Direct activation and temporal response properties of rabbit retinal ganglion cells following subretinal stimulation. *J Neurophysiol.* 2009;102(5):2982–93.
13. Dokos S. Computational Models of Neural Retina. In: Dieter J, Ranu J, editors. *Encyclopedia of Computational Neuroscience*: Springer; 2014. Doi: 10.1007/978-1-4614-7320-6_652-1
14. Luo YH, da Cruz L. A review and update on the current status of retinal prostheses (bionic eye). *Br Med Bull.* 2014;109:31–44.
15. Kamiyama Y, Ogura T, Usui S. Ionic current model of the vertebrate rod photoreceptor. *Vision Res.* 1996;36(24):4059–68.
16. Publio R, Oliveira RF, Roquea AC. A realistic model of rod photoreceptor for use in a retina network model. *Neurocomputing.* 2006;69(10–12):1020–4.
17. Kourennyi DE, Liu XD, Hart J, Mahmud F, Baldrige WH, Barnes S. Reciprocal modulation of calcium dynamics at rod and cone photoreceptor synapses by nitric oxide. *J Neurophysiol.* 2004;92(1):477–83.
18. Aoyama T, Kamiyama Y, Usui S. Simulation analysis of receptive-field size of retinal horizontal cells by ionic current model. *Visual Neurosci.* 2005;22(1):65–78.
19. Usui S, Kamiyama Y, Ishii H, Ikeno H. Reconstruction of retinal horizontal cell responses by the ionic current model. *Vision Res.* 1996;36(12):1711–9.
20. Shirahata T. Simulation of rabbit A-type retinal horizontal cell that generates repetitive action potentials. *Neurosci Lett.* 2008;439(1):116–8.
21. Usui S, Ishihara A, Kamiyama Y, Ishii H. Ionic current model of bipolar cells in the lower vertebrate retina. *Vision Res.* 1996;36(24):4069–76.
22. Steffen MA, Seay CA, Amini B, Cai YD, Feigenspan A, Baxter DA, Marshak DW. Spontaneous activity of dopaminergic retinal neurons. *Biophys J.* 2003;85(4):2158–69.
23. Shirahata T. The effect of variations in sodium conductances on pacemaking in a dopaminergic retinal neuron model. *Acta Biol Hung.* 2011;62(2):211–4.
24. Fohlmeister JF, Miller RF. Impulse encoding mechanisms of ganglion cells in the tiger salamander retina. *J Neurophysiol.* 1997;78(4):1935–47.
25. Fohlmeister JF, Coleman PA, Miller RF. Modeling the repetitive firing of retinal ganglion cells. *Brain research.* 1990;510(2):343–5.
26. Guo T, Tsai D, Suaning GJ, Lovell NH, Dokos S. Modeling normal and rebound excitation in mammalian retinal ganglion cells. *Conference Proceedings: Annual International Conference of the IEEE Engineering in Medicine and Biology Society.* 2012;2012:5506–9.
27. Kameneva T, Meffin H, Burkitt AN. Modelling intrinsic electrophysiological properties of ON and

- OFF retinal ganglion cells. *J Comput Neuroscience*. 2011;31(3):547–61.
28. Aidley DJ. The physiology of excitable cells, 2nd ed. Cambridge, UK: Cambridge University Press; 1979.
29. Hodgkin AL, Huxley AF. A quantitative description of membrane current and its application to conduction and excitation in nerve. *J Physiol*. 1952;117(4):500–44.
30. Fohlmeister JF, Miller RF. Mechanisms by which cell geometry controls repetitive impulse firing in retinal ganglion cells. *J Neurophysiol*. 1997;78(4):1948–64.
31. Fohlmeister JF. A nerve model of greatly increased energy-efficiency and encoding flexibility over the Hodgkin-Huxley model. *Brain Res*. 2009;1296:225–33.
32. Carras PL, Coleman PA, Miller RF. Site of action potential initiation in amphibian retinal ganglion cells. *J Neurophysiol*. 1992;67(2):292–304.
33. AlAbed A, Lovell NH, Suaning GJ, Dokos S. A continuum neuronal tissue model based on a two-compartmental representation of cells. Conference Proceedings: Annual International Conference of the IEEE Engineering in Medicine and Biology Society. 2013;2013:6543–6.
34. Boinagrov D, Loudin J, Palanker D. Strength-duration relationship for extracellular neural stimulation: numerical and analytical models. *J Neurophysiol*. 2010;104(4):2236–48.
35. Taylor GC, Coles JA, Eilbeck JC. Mathematical-modeling of weakly nonlinear pulses in a retinal neuron. *Chaos Soliton Fract*. 1995;5(3–4):407–13.
36. McCormick DA, Shu Y, Yu Y. Neurophysiology: Hodgkin and Huxley model—still standing? *Nature*. 2007;445(7123):1060–3.
37. Mainen ZF, Sejnowski TJ. Influence of dendritic structure on firing pattern in model neocortical neurons. *Nature*. 1996;382(6589):363–6.
38. Herz AVM, Gollisch T, Machens CK, Jaeger D. Modeling single-neuron dynamics and computations: A balance of detail and abstraction. *Science*. 2006;314(5796):80–5.
39. Fohlmeister JF, Cohen ED, Newman EA. Mechanisms and distribution of ion channels in retinal ganglion cells: using temperature as an independent variable. *J Neurophysiol*. 2010;103(3):1357–74.
40. Greenberg RJ, Velte TJ, Humayun MS, Scarlatis GN, de Juan E, Jr. A Comput model of electrical stimulation of the retinal ganglion cell. *IEEE Trans Bio-Med Eng*. 1999;46(5):505–14.
41. Jeng J, Tang S, Molnar A, Desai NJ, Fried SI. The sodium channel band shapes the response to electric stimulation in retinal ganglion cells. *J Neural Eng*. 2011;8(3):036022.
42. Tsai D, Chen S, Protti DA, Morley JW, Suaning GJ, Lovell NH. Responses of retinal ganglion cells to extracellular electrical stimulation, from single cell to population: model-based analysis. *PLoS One*. 2012;7(12):e53357.
43. Abramian M, Lovell NH, Morley JW, Suaning GJ, Dokos S. Activation of retinal ganglion cells following epiretinal electrical stimulation with hexagonally arranged bipolar electrodes. *J Neural Eng*. 2011;8(3):035004.
44. Sheasby BW, Fohlmeister JF. Impulse encoding across the dendritic morphologies of retinal ganglion cells. *J Neurophysiol*. 1999;81(4):1685–98.
45. Guo T, Tsai D, Morley JW, Suaning GJ, Lovell NH, Dokos S. Influence of cell morphology in a computational model of ON and OFF retinal ganglion cells. Conference Proceedings: Annual International Conference of the IEEE Engineering in Medicine and Biology Society. 2013;2013:4553–6.
46. Guo T, Tsai D, Sovilj S, Morley JW, Suaning GJ, Lovell NH, Dokos S. Influence of active dendrites on firing patterns in a retinal ganglion cell model. Conference Proceedings: Annual International Conference of the IEEE Engineering in Medicine and Biology Society. 2013;2013:4557–60.
47. Schachter MJ, Oesch N, Smith RG, Taylor WR. Dendritic spikes amplify the synaptic signal to enhance detection of motion in a simulation of the direction-selective ganglion cell. *PLoS Comput biology*. 2010;6(8):e1000899.
48. Guo T, Tsai D, Morley JW, Suaning GJ, Lovell NH, Dokos S. Cell-specific modeling of retinal ganglion cell electrical activity. Conference Proceedings: Annual International Conference of the IEEE Engineering in Medicine and Biology Society. 2013;2013:6539–42.
49. Abbas SY, Hamade KC, Yang EJ, Nawy S, Smith RG, Pettit DL. Directional summation in non-direction selective retinal ganglion cells. *PLoS Comput Biol*. 2013;9(3):e1002969.
50. Maturana MI, Kameneva T, Burkitt AN, Meffin H, Grayden DB. The effect of morphology upon electrophysiological responses of retinal ganglion cells: simulation results. *J Comput Neurosci*. 2013;DOI: 10.1007/s10827-013-0463-7.
51. Velte TJ, Masland RH. Action potentials in the dendrites of retinal ganglion cells. *J Neurophysiol*. 1999;81(3):1412–7.
52. Oesch N, Euler T, Taylor WR. Direction-selective dendritic action potentials in rabbit retina. *Neuron*. 2005;47(5):739–50.
53. Sivyer B, Williams SR. Direction selectivity is computed by active dendritic integration in retinal ganglion cells. 2013;16(12):1848–56.
54. Vigh J, Banvolgyi T, Wilhelm M. Amacrine cells of the anuran retina: morphology, chemical neuroanatomy, and physiology. *Microscopy Res Tech*. 2000;50(5):373–83.
55. Yang CY, Lukasiewicz P, Maguire G, Werblin FS, Yazulla S. Amacrine cells in the tiger salamander retina: morphology, physiology, and neurotransmitter identification. *J Comparative Neurol*. 1991;312(1):19–32.
56. Tukker JJ, Taylor WR, Smith RG. Direction selectivity in a model of the starburst amacrine cell. *Visual Neurosci*. 2004;21(4):611–25.
57. Miller RF, Staff NP, Velte TJ. Form and function of ON-OFF amacrine cells in the amphibian retina. *J Neurophysiol*. 2006;95(5):3171–90.
58. Resatz S, Rattay F. A model for the electrically stimulated retina. *Math Comp Model Dyn*. 2004;10(2):93–106.

59. Rattay F, Resatz S, Lutter P, Minassian K, Jilge B, Dimitrijevic MR. Mechanisms of electrical stimulation with neural prostheses. *Neuromodulation*. 2003;6(1):42–56.
60. Rattay F, Resatz S. Effective electrode configuration for selective stimulation with inner eye prostheses. *IEEE Trans Bio-Med Engineering*. 2004;51(9):1659–64.
61. Schiefer MA, Grill WM. Sites of neuronal excitation by epiretinal electrical stimulation. *IEEE T Neur Sys Reh*. 2006;14(1):5–13.
62. Poznanski RR. Modelling the electrotonic structure of starburst amacrine cells in the rabbit retina: a functional interpretation of dendritic morphology. *Bull Math Biol*. 1992;54(6):905–28.
63. Enciso G, Rempe M, Dmitriev AV, Gavrikov KE, Terman D, Mangel SC. A model of direction selectivity in the starburst amacrine cell network. *J Comput Neurosci*. 2010;28(3):567–78.
64. Mennerick S, Zenisek D, Matthews G. Static and dynamic membrane properties of large-terminal bipolar cells from goldfish retina: experimental test of a compartment model. *J Neurophysiol*. 1997;78(1):51–62.
65. Smith RG. Simulation of an anatomically defined local circuit: the cone-horizontal cell network in cat retina. *Visual Neurosci*. 1995;12(3):545–61.
66. van Elburg RA, van Ooyen A. Impact of dendritic size and dendritic topology on burst firing in pyramidal cells. *PLoS Comput Biol*. 2010;6(5):e1000781.
67. Ristanovic D, Milosevic NT, Jelinek HF, Stefanovic IB. Mathematical modelling of neuronal dendritic branching patterns in two dimensions: application to retinal ganglion cells in the cat and rat. *Biol Cybernetics*. 2009;100(2):97–108.
68. Wong RC, Cloherty SL, Ibbotson MR, O'Brien BJ. Intrinsic physiological properties of rat retinal ganglion cells with a comparative analysis. *J Neurophysiol*. 2012;108(7):2008–23.
69. O'Brien BJ, Isayama T, Richardson R, Berson DM. Intrinsic physiological properties of cat retinal ganglion cells. *J Physiol*. 2002;538(Pt 3):787–802.
70. Rockhill RL, Daly FJ, MacNeil MA, Brown SP, Masland RH. The diversity of ganglion cells in a mammalian retina. *J Neurosci*. 2002;22(9):3831–43.
71. Roth BJ, Wikswo JP. Electrical-stimulation of cardiac tissue—a bidomain model with active membrane-properties. *IEEE Trans Bio-Med Eng*. 1994;41(3):232–40.
72. Henriquez CS. Simulating the electrical behavior of cardiac tissue using the bidomain model. *Crit Rev Biomed Eng*. 1993;21(1):1–77.
73. Altman KW, Plonsey R. Point-source nerve bundle stimulation—effects of fiber diameter and depth on simulated excitation. *IEEE Trans Bio-Med Eng*. 1990;37(7):688–98.
74. Martinek J, Stickler Y, Reichel M, Mayr W, Rattay F. A novel approach to simulate Hodgkin–Huxley-like excitation with COMSOL multiphysics. *Artif Organs*. 2008;32(8):614–9.
75. Brindley GS. The passive electrical properties of the frog's retina, choroid and sclera for radial fields and currents. *J Physiol*. 1956;134(2):339–52.
76. Yin S, Lovell NH, Suaning GJ, Dokos S. A continuum model of the retinal network and its response to electrical stimulation. *Conference Proceedings: Annual International Conference of the IEEE Engineering in Medicine and Biology Society*. 2010;2010:2077–80.
77. Dokos S, Suaning GJ, Lovell NH. A bidomain model of epiretinal stimulation. *Neural Systems and Rehabilitation Engineering: IEEE Trans*. 2005;13(2):137–46.
78. Joarder SA, Abramian M, Suaning GJ, Lovell NH, Dokos S. A continuum model of retinal electrical stimulation. *J Neural Eng*. 2011;8(6):066006.
79. Abramian M, Lovell NH, Habib A, Morley JW, Suaning GJ, Dokos S. Quasi-monopolar electrical stimulation of the retina: a computational modelling study. *J Neural Eng*. 2014;11(2):025002.
80. Matteucci PB, Chen SC, Tsai D, Dodds CWD, Dokos S, Morley JW, Lovell NH, Suaning GJ. Current steering in retinal stimulation via a quasimonopolar stimulation paradigm. *Invest Ophthalm Vis Sci*. 2013;54(6):4307–20.
81. Yin S, Lovell NH, Suaning GJ, Dokos S. Continuum model of light response in the retina. *Conference Proceedings: Annual International Conference of the IEEE Engineering in Medicine and Biology Society*. 2011;2011:908–11.
82. Pillow JW, Paninski L, Uzzell VJ, Simoncelli EP, Chichilnisky EJ. Prediction and decoding of retinal ganglion cell responses with a probabilistic spiking model. *J Neurosci*. 2005;25(47):11003–13.
83. Pillow JW, Shlens J, Paninski L, Sher A, Litke AM, Chichilnisky EJ, Simoncelli EP. Spatio-temporal correlations and visual signalling in a complete neuronal population. *Nature*. 2008;454(7207):995–99.
84. Curlander JC, Marmarelis VZ. A linear spatiotemporal model of the light-to-bipolar cell system and its response characteristics to moving bars. *Biol Cybernetics*. 1987;57(6):357–63.
85. Teeters J, Jacobs A, Werblin F. How neural interactions form neural responses in the salamander retina. *J Comput Neurosci*. 1997;4(1):5–27.
86. Wohrer A, Kornprobst P. Virtual retina: a biological retina model and simulator, with contrast gain control. *J Comput Neurosci*. 2009;26(2):219–49.
87. van Hateren JH, Snippe HP. Simulating human cones from mid-mesopic up to high-photopic luminances. *J Vision*. 2007;7(4):1–11.
88. Shah S, Levine MD. Visual information processing in primate cone pathways. I. A model. *Systems, Man, and Cybernetics, Part B, IEEE Trans*. 1996;26(2):259–74.
89. Shah S, Levine MD. Visual information processing in primate cone pathways. II. Experiments. *Systems, Man, and Cybernetics, Part B, IEEE Trans*. 1996;26(2):275–89.

90. Hamer RD, Nicholas SC, Tranchina D, Lamb TD, Jarvinen JLP. Toward a unified model of vertebrate rod phototransduction. *Visual Neurosci.* 2005;22(4):417–36.
91. Lamb TD, Pugh EN, Jr. A quantitative account of the activation steps involved in phototransduction in amphibian photoreceptors. *J Physiol.* 1992;449:719–58.
92. Hood DC, Shady S, Birch DG. Heterogeneity in retinal disease and the computational model of the human-rod response. *Optics Image Sci.* 1993;10(7):1624–30.
93. Juusola M, Weckstrom M, Uusitalo RO, Korenberg MJ, French AS. Nonlinear models of the first synapse in the light-adapted fly retina. *J Neurophysiol.* 1995;74(6):2538–47.
94. Victor JD. The dynamics of the cat retinal Y-cell subunit. *J Physiol-London.* 1988;405:289–320.
95. Victor JD. The dynamics of the cat retinal X-cell center. *J Physiol-London.* 1987;386:219–46.
96. Keat J, Reinagel P, Reid RC, Meister M. Predicting every spike: a model for the responses of visual neurons. *Neuron.* 2001;30(3):803–17.
97. Berry MJ, 2nd, Brivanlou IH, Jordan TA, Meister M. Anticipation of moving stimuli by the retina. *Nature.* 1999;398(6725):334–8.
98. Baccus SA, Olveczky BP, Manu M, Meister M. A retinal circuit that computes object motion. *J Neurosci.* 2008;28(27):6807–17.
99. Smith RG, Freed MA, Sterling P. Microcircuitry of the dark-adapted cat retina—functional architecture of the rod cone network. *J Neurosci.* 1986;6(12):3505–17.
100. Robson JG, Frishman LJ. Photoreceptor and bipolar-cell contributions to the cat electroretinogram: A kinetic model for the early part of the flash response. *Optics Image Sci.* 1996;13(3):613–22.
101. Publio R, Oliveira RF, Roque AC. A computational study on the role of gap junctions and rod I-h conductance in the enhancement of the dynamic range of the retina. *PloS One.* 2009;4(9):e6970.
102. Arguello E, Silva R, Huerta M, Castillo C. New trends in computational modeling: a neuroid-based retina model. *Conference Proceedings: Annual International Conference of the IEEE Engineering in Medicine and Biology Society.* 2013;2013:4561–4.
103. Cottaris NP, Elfar SD, Iezzi R, Abrams GW. How the retinal network reacts to epiretinal stimulation to form the prosthetic visual input to the cortex: computational modeling of a degenerated retina. *Invest Ophth Vis Sci.* 2005;46:S74–90.
104. Smith RG, Vardi N. Simulation of the Aii amacrine cell of mammalian retina—functional consequences of electrical coupling and regenerative membrane-properties. *Visual Neurosci.* 1995;12(5):851–60.
105. Publio R, Ceballos CC, Roque AC. Dynamic range of vertebrate retina ganglion cells: importance of active dendrites and coupling by electrical synapses. *PloS One.* 2012;7(10):e48517.
106. Bomash I, Roudi Y, Nirenberg S. A virtual retina for studying population coding. *PloS One.* 2013;8(1):e53363.
107. Hennig MH, Funke K, Worgotter F. The influence of different retinal subcircuits on the nonlinearity of ganglion cell behavior. *J Neurosci.* 2002;22(19):8726–38.
108. Rekeczky C, Roska B, Nemeth E, Werblin FS. The network behind spatio-temporal patterns: building low-complexity retinal models in CNN based on morphology, pharmacology and physiology. *Int J Circ Theor App.* 2001;29(2):197–239.
109. Herrmann R, Heflin SJ, Hammond T, Lee B, Wang J, Gainetdinov RR, Caron MG, Eggers ED, Frishman LJ, McCall MA, Arshavsky VY. Rod vision is controlled by dopamine-dependent sensitization of rod bipolar cells by GABA. *Neuron.* 2011;72(1):101–10.
110. Klaassen LJ, Sun ZY, Steijaert MN, Bolte P, Fahrenfort I, Sjoerdsma T, Klooster J, Claassen Y, Shields CR, Ten Eikelder HMM, Janssen-Bienhold U, Zoidl G, McMahon DG, Kamermans M. Synaptic Transmission from Horizontal Cells to Cones Is Impaired by Loss of Connexin Hemichannels. *Plos Biol.* 2011; 9(7): e1001107
111. Jackman SL, Babai N, Chambers JJ, Thoreson WB, Kramer RH. A positive feedback synapse from retinal horizontal cells to cone photoreceptors. *Plos Biol.* 2011;9(5).
112. Freed MA. Parallel cone bipolar pathways to a ganglion cell use different rates and amplitudes of quantal excitation. *J Neurosci.* 2000;20(11):3956–63.
113. Dreosti E, Esposti F, Baden T, Lagnado L. *In vivo* evidence that retinal bipolar cells generate spikes modulated by light. *Nature Neurosci.* 2011;14(8):951–2.
114. Miller RF, Stenback K, Henderson D, Sikora M. How voltage-gated ion channels alter the functional properties of ganglion and amacrine cell dendrites. *Arch Italiennes Biol.* 2002;140(4):347–59.
115. Tabata T, Ishida AT. Transient and sustained depolarization of retinal ganglion cells by Ih. *J Neurophysiol.* 1996;75(5):1932–43.
116. Lee SC, Ishida AT. Ih without Kir in adult rat retinal ganglion cells. *J Neurophysiol.* 2007;97(5):3790–9.
117. Traub RD, Contreras D, Cunningham MO, Murray H, LeBeau FE, Roopun A, Bibbig A, Wilent WB, Higley MJ, Whittington MA. Single-column thalamocortical network model exhibiting gamma oscillations, sleep spindles, and epileptogenic bursts. *J Neurophysiol.* 2005;93(4):2194–232.
118. Werginz P, Fried SI, Rattay F. Influence of the sodium channel band on retinal ganglion cell excitation during electric stimulation—a modeling study. *Neurosci.* 2014;266:162–77.
119. Velte TJ, Miller RF. Spiking and nonspiking models of starburst amacrine cells in the rabbit retina. 1997;14(06):1073–88.
120. Borg-Graham LJ. The computation of directional selectivity in the retina occurs presynaptic to the ganglion cell. *Nature Neurosci.* 2001;4(2):176–83.

121. Freed MA, Smith RG, Sterling P. Computational model of the on-alpha ganglion-cell receptive-field based on bipolar cell circuitry. *P Natl Acad Sci USA*. 1992;89(1):236–40.
122. Velle TJ, Miller RF. Dendritic integration in ganglion cells of the mudpuppy retina. *Visual Neurosci*. 1995;12(1):165–75.
123. Ogura T, Satoh TO, Usui S, Yamada M. A simulation analysis on mechanisms of damped oscillation in retinal rod photoreceptor cells. *Vision Res*. 2003;43(19):2019–28.
124. Al Abed A, Yin S, Suaning GJ, Lovell NH, Dokos S. A Convolution based method for calculating inputs from dendritic fields in a continuum model of the retina. *Conference Proceedings: Annual International Conference of the IEEE Engineering in Medicine and Biology Society*. 2012;2012:215–8.
125. Boinagrov D, Pangratz-Fuehrer S, Suh B, Mathieson K, Naik N, Palanker D. Upper threshold of extracellular neural stimulation. *J Neurophysiol*. 2012;108(12):3233–8.
126. Hennig MH, Worgotter F. Effects of fixational eye movements on retinal ganglion cell responses: a modeling study. *Front Comput Neurosci*. 2007. Doi: 10.3389/Neuro.10/002.2007.
127. Borst A, Flanagan VL, Sompolinsky H. Adaptation without parameter change: dynamic gain control in motion detection. *P Natl Acad Sci USA*. 2005;102(17):6172–6.
128. Baylor DA, Hodgkin AL, Lamb TD. Reconstruction of the electrical responses of turtle cones to flashes and steps of light. *J Physiol*. 1974;242(3):759–91.
129. Vallerger S, Covacci R, Pottala EW. Artificial cone responses—a computer-driven hardware model. *Vision Res*. 1980;20(5):453–7.
130. Usui S, Mitarai G, Sakakibara M. Discrete nonlinear reduction model for horizontal cell response in the carp retina. *Vision Res*. 1983;23(4):413–20.
131. Robson JG, Frishman LJ. Response linearity and kinetics of the cat retina: the bipolar cell component of the dark-adapted electroretinogram. *Visual Neurosci*. 1995;12(5):837–50.
132. Saglam M, Hayashida Y, Murayama N. A retinal circuit model accounting for wide-field amacrine cells. *Cogn Neurodynamics*. 2009;3(1):25–32.
133. Cai CF, Liang PJ, Zhang PM. A simulation study on the encoding mechanism of retinal ganglion cell. *Lect N Bioinformat*. 2007;4689:470–9.
134. Yin S, Dokos S, Lovell NH. Bidomain modeling of neural tissue. In: He B, Editor. *Neural engineering*. New York: Springer; 2013. p. 389–404.
135. Wang L, Liu SQ, Ou SX. Numerical simulation of neuronal spike patterns in a retinal network model. *Neural Regen Res*. 2011;6(16):1254–60.
136. Haderer KP, Kuhn D. Stationary states of the Hartline–Ratliff model. *Biological Cybernetics*. 1987;56(5–6):411–7.
137. Rall W. Branching dendritic trees and motoneuron membrane resistivity. *Exp Neurol*. 1959;1(5):491–527.